

OPEN

Gender-specific changes in energy metabolism and protein degradation as major pathways affected in livers of mice treated with ibuprofen

Shuchita Tiwari¹, Manish Mishra¹, Michelle R. Salemi², Brett S. Phinney², Joanne L. Newens¹ & Aldrin V. Gomes^{1,3*}

Ibuprofen, an inhibitor of prostanoid biosynthesis, is a common pharmacological agent used for the management of pain, inflammation and fever. However, the chronic use of ibuprofen at high doses is associated with increased risk for cardiovascular, renal, gastrointestinal and liver injuries. The underlying mechanisms of ibuprofen-mediated effects on liver remain unclear. To determine the mechanisms and signaling pathways affected by ibuprofen (100 mg/kg/day for seven days), we performed proteomic profiling of male mice liver with quantitative liquid chromatography tandem mass spectrometry (LC-MS/MS) using ten-plex tandem mass tag (TMT) labeling. More than 300 proteins were significantly altered between the control and ibuprofen-treated groups. The data suggests that several major pathways including (1) energy metabolism, (2) protein degradation, (3) fatty acid metabolism and (4) antioxidant system are altered in livers from ibuprofen treated mice. Independent validation of protein changes in energy metabolism and the antioxidant system was carried out by Western blotting and showed sex-related differences. Proteasome and immunoproteasome activity/expression assays showed ibuprofen induced gender-specific proteasome and immunoproteasome dysfunction in liver. The study observed multifactorial gender-specific ibuprofen-mediated effects on mice liver and suggests that males and females are affected differently by ibuprofen.

Ibuprofen, a propionic acid derivative, is the most common over-the-counter nonsteroidal anti-inflammatory (NSAID) drug used to treat fever, pain, inflammation and many other disorders¹. It has been included as a major medicine in the *Essential Drugs List* of the World Health Organization². Ibuprofen at low over-the-counter doses (800–1200 mg/day) is used to treat muscular aches, backaches, toothaches, and fever. At higher doses (1800–2400 mg/day), ibuprofen is prescribed for the treatment of chronic conditions such as osteoarthritis, rheumatoid arthritis, and ankylosing spondylitis³. Ibuprofen is a non-selective inhibitor of the cyclo-oxygenase (COX) isozymes COX-1 and COX-2 that converts arachidonic acid into prostaglandins including thromboxane and prostacyclin¹. The anti-inflammatory, antipyretic and analgesic effects of ibuprofen are mediated through the inhibition of prostaglandins E2 (PGE2) and I2 (PGI2) production by blocking COX activity¹. Both PGE2 and PGI2 are pro-inflammatory prostanoids that increase vascular permeability, promote leukocyte infiltration and increase edema formation⁴. The clearance of ibuprofen is mediated through oxidative metabolism by multiple cytochrome P450 (CYP) enzymes (CYP2C9, CYP2C8) to inactive primary metabolites including 3-hydroxy-ibuprofen, carboxy ibuprofen and 2-hydroxy-ibuprofen^{5,6}. Most of the ibuprofen is metabolized in liver, while only a small percentage of unchanged drug is excreted in the urine⁵.

The liver plays a key role in energy metabolism and is essential for whole body homeostasis via the regulation of glucose, lipid, and amino acid metabolism⁷. While various NSAIDs, including ibuprofen are considered safe to sell without prescriptions, they have the potential to cause adverse side effects. Adverse reactions associated

¹Department of Neurobiology, Physiology, and Behavior, University of California, Davis, CA, USA. ²Proteomics Core Facility, University of California, Davis, CA, USA. ³Department of Physiology and Membrane Biology, University of California, Davis, CA, USA. *email: avgomes@ucdavis.edu

with NSAIDs treatment can affect the gastrointestinal system, increase blood pressure and cause cardiac, renal and hepatic injuries^{8,9}. Treatment with aspirin to a patient with pericarditis was reported to develop acute liver injury¹⁰. The long term administration (4 weeks) of aspirin and ibuprofen to rats increased mitochondrial number, altered liver mitochondria ultrastructure and increased the metabolic activity of the CYP450 enzymes¹¹. Previous research in our laboratory has suggested that physiological concentrations of NSAIDs (diclofenac, naproxen and meclofenamate sodium) cause mitochondrial and proteasome dysfunction in cardiac tissue^{12,13}.

To investigate the mechanisms by which ibuprofen affect mouse liver, a quantitative LC-MS/MS technique using tandem mass tag (TMT) labeling was carried out to measure whole liver proteome changes after short-term (7 days) treatment of ibuprofen (100 mg/kg/day). Although the mass spectrometry was initially carried out on livers from male mice, we hypothesized that ibuprofen would cause similar effects on livers from female mice. To determine if ibuprofen has the same effect in male and female mice, biological assays and Western blots were carried out on ibuprofen and vehicle treated mice. The amount of ibuprofen utilized in mice would be equivalent to a human taking approximately 486 mg/day, significantly less than the 1200 mg/day maximum over-the-counter dosage recommended. Ibuprofen at a moderate amount (100 mg/kg/day) affected more proteins and pathways in mice liver than expected, including glycolysis, protein degradation, fatty acid metabolism and antioxidant system. Biological assays and Western blotting exposed significant gender-specific differences in livers from ibuprofen treated males and females relative to their respective controls.

Materials and Methods

Animal studies. Aged matched male and female C57BL/6J mice were used for the study. The study protocol was approved by Institutional Animal Care and Use Committee (IACUC) of the University of California, Davis. Mice were maintained at controlled temperature and humidity and had free access to food and water. Methods used for all mice were performed in accordance with UC Davis IACUC guidelines and regulations. Ibuprofen was administered orally in drinking water at a concentration 100 mg/kg/day for seven days. The average water consumption by mice was measured to ensure that mice got the appropriate levels of ibuprofen. The ibuprofen dose used in this study was similar to the concentrations used in previous studies^{1,14,15}. This dosage was chosen as it approximates to a human taking 486 mg/day which is between two to three dosages of 200 mg/day. In humans the recommended dosages of ibuprofen are 200 to 400 mg orally every 4 to 6 hours as needed with a maximum dose of 1200 mg/day for over-the-counter use. A 1200 mg/day ibuprofen dose (20 mg/kg/day, assuming an average human weight of 60 kg), would correspond to a treatment of 246.9 mg/kg/day in mice using the dose translation equation (Human equivalent dose (HED) = Animal Dose (mg/kg) × Animal Km (3 for mouse)/Human Km (37 for human)¹⁶. The maximum human prescription dose (3200 mg/day) would correspond to a 658.4 mg/kg/day dose in mice. Hence, the amount of ibuprofen used in this study (100 mg/kg/day) would approximate to a moderate daily dose of ibuprofen in humans. At the end of the study the mice were euthanized, and the livers were collected and quickly washed twice in ice-cold phosphate-buffered saline (PBS). The tissues were then frozen and pulverized in liquid nitrogen. The pulverized tissue was collected in clean microcentrifuge tubes and stored at -80°C until needed.

LC-MS/MS using 10-plex TMT proteomics. *Sample preparation.* Pulverized liver tissue (20 mg aliquot) were homogenized in lysis buffer (8 M urea, 50 mM TEAB (triethyl ammonium bicarbonate), pH 8) followed by sonication (at level 5; three cycles for 10 sec with 30 sec wait in between on ice) to reduce sample viscosity. The lysate was centrifuged at 15,000 g for 15 minutes at 4°C , and the supernatant was separated. The protein concentration of the supernatant was measured using Bicinchoninic Acid (BCA) protein assay. 100 μg (100 μl) of protein sample was removed and 5 μl of the 200 mM TCEP (tris(2-carboxyethyl) phosphine) added and incubated at 55°C for 1 hr in a heat block. After that, 5 μl of 375 mM iodoacetamide was added to the sample and incubated for 30 minutes sheltered from light at room temp. The samples were acetone precipitated using pre-chilled (-20°C) 6 volumes ($\sim 600\ \mu\text{l}$) of acetone overnight. Next day samples were centrifuged at 10,000 xg for 10 minutes at 4°C , the supernatant was discarded, and pellet was air dried.

Digestion of protein samples. The acetone-precipitated protein pellet was resuspended in 100 μl of 50 mM ammonium bicarbonate (NH_4CO_3). 2.5 μl of trypsin (i.e. 2.5 μg) per 100 μg of protein was added to each sample and were incubated overnight at 37°C . The digested samples were lyophilized with a speedvac and resuspended in 0.1% trifluoroacetic acid (TFA) and 5% acetonitrile.

TMT 10-plex peptide labeling. TMT label reagents were allowed to equilibrate to room temperature (RT) and anhydrous acetonitrile was added to each tube. 21.6 μl of the TMT label reagents were added to each 20 μg of samples and were incubated for 1 hr at RT. The reaction was quenched by adding 8 μl of 5% hydroxylamine to the labeled samples and were incubated for 30 minutes at RT. All TMT labeled samples were combined in equal amounts in a new tube (200 μg) and were run on Mass spec after fractionation.

TMT labeled samples were then reconstituted in 0.1% TFA and the pH adjusted to 2 with 10% TFA¹⁷. The combined sample (200 μg) was separated into 8 fractions by Pierce High pH Reverse-Phase Peptide Fractionation kit (Thermo Scientific) with an extra wash before separation to remove extra labels¹⁷. The eight fractions were dried almost to completion.

LC-MS/MS. LC separation was done on a Dionex Nano Ultimate 3000 (Thermo Scientific) with a Thermo Easy-Spray source¹⁷. The digested peptides were reconstituted in 2% acetonitrile/0.1% TFA and 5 μl of each sample was loaded onto a PepMap 100 \AA 3U 75 μm \times 20 mm reverse-phase trap where they were desalted online before being separated on a 100 \AA 2U 50-micron \times 150 mm PepMap EasySpray reverse-phase column¹⁷. Peptides were eluted using a 180-minute gradient of 0.1% formic acid (A) and 80% acetonitrile (B) with a flow rate of

200 nL/min. The separation gradient was run with 2% to 5% B over 1 minute, 5% to 10% B over 9 minutes, 10% to 20% B over for 27 minutes, 20% to 35% B over 10 minutes, 35% B to 99% B over 10 minutes, a 2 minute hold at 99% B, and finally 99% B to 2% B held at 2% B for 5 minutes¹⁷.

MS3 synchronous precursor selection workflow. Mass spectra were collected on a Fusion Lumos mass spectrometer (Thermo Fisher Scientific) in a data-dependent MS3 synchronous precursor selection (SPS) method¹⁷. MS1 spectra were acquired in the Orbitrap, 120 K resolution, 50 ms max inject time, 5×10^5 max inject time. MS2 spectra were acquired in the linear ion trap with a 0.7 Da isolation window, CID fragmentation energy of 35%, turbo scan speed, 50 ms max inject time, 1×10^4 automatic gain control (AGC) and maximum parallelizable time turned on¹⁷. MS2 ions were isolated in the ion trap and fragmented with a HCD energy of 65%. MS3 spectra were acquired in the orbitrap with a resolution of 50K and a scan range of 100–500 Da, 105 ms max inject time and 1×10^5 AGC¹⁷.

TMT data analysis (Quantitative data analysis). The use of 5 ibuprofen treated samples and 5 vehicle treated samples for the TMT 10 plex experiment animals and a [1.2]-fold cut-off was based on power analysis taking into account that isobaric-labeled LC-MS/MS quantitative measurements are known to be compressed by various factors. These factors include ratio compression and cause an underestimation of changes in relative abundance of proteins across samples¹⁸. This underestimation was $\geq 50\%$ for other isobaric labeling-based experiments¹⁹. In these experiments a protein that was upregulated by 2.4 gave a measurement of only 1.2¹⁹. As such the [1.2]-fold change for the TMT experiment was considered to be equivalent to a [1.5]-fold change. For power analysis (using online program <https://www.stat.ubc.ca/rollin/stats/ssize/n2.html>), when sigma (common standard deviation) was set at 25%, power at 0.80 and $\alpha = 0.05$, a minimum of 4 mice in each group was needed.

Raw files were processed with Proteome Discoverer 2.2 (Thermo Scientific) using the default MS3 SPS method with the following modifications for importation into Scaffold Q+. Target Decoy PSM validator was used instead of Percolator and Maximum Delta Cn was set to 1. All MS/MS samples were analyzed using Sequest HT to search all mouse sequences from Uniprot (<https://www.uniprot.org/teomes/UP000000589>) and 110 common laboratory contaminants (<http://thegpm.org.crap>) plus an equal number of reverse decoy sequences assuming the digestion enzyme trypsin¹⁷. Sequest-HT was searched with a fragment ion mass tolerance of 0.20 Da and a parent ion tolerance of 10.0 PPM. Carbamidomethyl of cysteine and TMT10 plex of lysine were specified in Sequest-HT as fixed modifications¹⁷. Oxidation of methionine and acetyl of the n-terminus were specified in Sequest-HT as variable modifications.

Scaffold Q+ (version Scaffold_4.9.0, Proteome Software Inc., Portland, OR) was used to quantitate Label Based Quantitation (iTRAQ, TMT, SILAC, etc.) peptide and protein identifications. Peptide identifications were accepted¹⁷ with a decoy false discovery rate (FDR) cutoff of less than 0.2%. Protein identifications were accepted if they could be established with at least 2 unique identified peptides. Proteins that contained similar peptides and could not be differentiated based on MS/MS analysis alone were grouped to satisfy the principles of parsimony. Proteins sharing significant peptide evidence were grouped into clusters²⁰. Channels were corrected as described in the supplementary text²¹. Normalization was performed iteratively (across samples and spectra) on intensities, as described in Statistical Analysis of Relative Labeled Mass Spectrometry Data from Complex Samples using ANOVA²². Medians were used for averaging. Spectra data were log-transformed and weighted by an adaptive intensity weighting algorithm. Of 80801 spectra in the experiment at the required thresholds, 79849 (99%) were incorporated into the quantitation and 4109 proteins were detected in 3700 clusters with 6 decoys (FDR 0.1%). 477 proteins were found to be differentially expressed (Supplemental Table 1), of which 302 proteins had a minimum fold change of 1.2 (Supplemental Table 2). All the analysis was carried out using the information from the 302 differentially expressed proteins (0.3% FDR) which show $\geq [1.2]$ -fold change.

26S proteasome activity assay. Briefly, pulverized liver samples (20 mg aliquot) were homogenized in 26 S proteasome lysis buffer (50 mM Tris, 150 mM sodium chloride (NaCl), 1 mM ethylenediaminetetraacetic acid (EDTA), 5 mM magnesium chloride (MgCl_2) [pH 7.5]) with a hand-held Potter-Elvehjem homogenizer. The supernatant containing the proteasomes were separated after centrifugation at 12,000 xg for 15 min at 4 °C and were quantified and diluted to 1 $\mu\text{g}/\mu\text{L}$ concentration with proteasome lysis buffer. The $\beta 5$ (chymotrypsin-like), $\beta 2$ (trypsin-like) and $\beta 1$ (caspase-like) activities were assayed using 20 μg of protein. The assays were carried out in a total volume of 100 μL per well in a black 96-well plate. The adenosine triphosphate (ATP)-dependent 26 S assays were performed using 100 μM ATP in the absence and presence of a specific proteasome inhibitor: 10 μM bortezomib ($\beta 5$ activity) and 100 μM bortezomib ($\beta 1$ and $\beta 2$ activities). Specific fluorescence-tagged substrates for each proteasomal β subunits (Enzo Life Sciences, NY, USA): Z-LLE-AMC for $\beta 1$, Boc-LSTR-AMC for $\beta 2$ and Suc-LLVY-AMC for $\beta 5$ were used to initiate the reaction [27–30]. Proteasomal activities were measured at an excitation wavelength of 390 nm and an emission wavelength of 460 nm using a Fluoroskan Ascent fluorometer (Thermo Electron, MA) for every 15 min up to 120 min. Controls to validate the inhibitors used for these experiments are shown in Supplementary Fig. 1, and more extensive details about the proteasome assays have been previously published²³.

Immunoproteasome activity. 20 μg of liver samples from ibuprofen-treated and control animals were incubated with immunoproteasome buffer (50 mM Tris, 5 mM MgCl_2 , 20 mM potassium chloride (KCl), 1 mM DTT (freshly added), pH 7.5), and inhibitor or an equal volume of dimethyl sulfoxide (DMSO) for 20 min at room temperature. The specific inhibitors for $\beta 5$ 20 μM ONX-0914 (Abmole Bioscience Inc., Houston, TX, Cat. No. M2071) and for $\beta 1$ 50 μM bortezomib was used to evaluate the specificity of the assay. The 25 μM fluorogenic substrates ANW-R110 (AAT Bioquest, Inc, CA) for $\beta 5$ and (Ac-Ala-Asn-Trp)2-R110 (AAT Bioquest, Cat. No. 13455)

for $\beta 1i$ were used to initiate the reaction. The fluorescence intensity was measured every 5 mins for 60 min at an excitation of 498 nm and an emission of 520 nm at 37 °C in a Tecan Infinite M1000.

Catalase activity assay. 10 μ g of mice liver was homogenized in 1.15% KCl using a Dounce homogenizer. The samples were centrifuged at 12,000 rpm for 15 minutes. The supernatant was extracted and diluted with 50 mM phosphate buffer pH 7.0. The colorimetric assay to measure catalase activity in liver samples was done by using Sigma-Aldrich Catalase Assay Kit (Cat. CAT100). This assay in the presence of hydrogen peroxide (H_2O_2) and horseradish peroxidase (HRP) uses a substituted phenol (3,5-dichloro-2-hydroxybenzenesulfonic acid) that combines with 4-aminoantipyrine to form a red quinoneimine dye. All solutions were prepared as instructed by the manufacturer. Briefly, this assay measured the H_2O_2 substrate that remains after the catalase action. In first step, catalase via its catalytic pathway converted H_2O_2 to water and oxygen, and the reaction was stopped using sodium azide. Next, a small volume of reaction mix is then analyzed for the amount of H_2O_2 remaining by a colorimetric method. The absorbance was measured using a spectrophotometer at 520 nm, and the actual concentration was measured using Beer's Law: $[H_2O_2]$ (mM) = $A_{240}/0.0436$.

Hydrogen peroxide (H_2O_2) assay. H_2O_2 assay was performed using Sigma Aldrich Fluorimetric Hydrogen Peroxide Assay Kit, (Cat. # MAK165). All steps were carried out as per manufacturer's instructions. The assay is based on the peroxidase substrate that reacts with H_2O_2 to generate a red fluorescent product that can be analyzed by a fluorescent microplate reader. Briefly, controls, standards, and samples were added to the wells followed by the addition of a master mix that contains red peroxidase substrate, peroxidase and assay buffer. The plate was incubated for 15 minutes at room temperature protected from light. The fluorescence intensity was measured at excitation = 540 and emission = 590 nm.

Western blotting. *Sample preparation.* Pulverized liver tissue (20 mg) was homogenized in ice cold 1x RIPA buffer (50 mM Tris, 150 mM NaCl, 1% NP40, 0.5% sodium deoxycholate and 0.1% sodium dodecyl sulfate (SDS), pH 8) using a glass dounce homogenizer. The homogenates were centrifuged at 12,000 xg for 15 min at 4 °C. The supernatants were separated and quantified using the BCA protein assay (Bio-Rad, Cat. #500-0119) and were diluted to equal protein concentrations. Liver samples were then mixed with 4X Laemmli sample buffer (8% SDS, 40% glycerol, 0.4% bromophenol blue, 240 mM Tris, pH 6.8) with freshly added β -mercaptoethanol and were heated for 5 mins at 95 °C.

Electrophoresis and western blotting. Equal amounts of protein (20 μ g) were separated on 4–20% 18-well TGX precast gels (Cat. # 567–1094, Bio-Rad) and were transferred to a nitrocellulose membrane (Trans-Blot Turbo Midi Nitrocellulose, #170–4159, Bio-Rad) using the Trans-Blot Turbo Transfer System (Cat # 170–4155, Bio-Rad). The membranes were then stained with Ponceau S and imaged to serve as a loading control for total protein normalization of Western blots. Thereafter the membrane was blocked with 3% nonfat dry milk (NFM) (Cat. # 170–6404, Bio-Rad) in Tris-buffered saline (TBS) (50 mM Tris, 150 mM NaCl, pH 7.5) containing 0.05% (wt/vol) Tween 20 (TBST) at room temperature. The membranes were then incubated overnight at 4 °C with the following 14 primary antibodies diluted to 1:2000 in 1% TBST: mouse anti-CYP1A2 (sc-53614), mouse anti-PFK-1 (sc-166722), mouse anti-fatty acid synthase (A-5) (sc-55580), mouse anti-PKLR (sc-133222), mouse anti-GSTM1 (sc-517262), mouse anti-CROT (H-1)(sc-365976), mouse anti-PROHIBITIN 2 (A-2) (sc-133094), mouse anti-ATP5F1 (C-12) (sc-514419), mouse anti-CYP4A1(clo1) (sc-53248), mouse anti-PKM (C-11) (sc-365684), mouse anti-GSTT2 (D-1) (sc-514667), mouse anti-FAAH (27- γ) (sc-100739), mouse anti-17- β HSD2 (E-7) (sc-374150), mouse anti-GSTA1/2/5 (E-6) (sc-398714), mouse anti-ETFDH (D-2) (sc-515202), mouse anti-LFABP (C-4) (sc-374537), mouse anti-LMP2, $\beta 1i$ (A-1) (sc-271354, LOT#B1611), mouse anti-MECL-1(71P6) $\beta 2i$ (sc-130295) (all from Santa Cruz), mouse anti- $\beta 5i$ (1:2000, custom made by Abgent), and rabbit anti-PSMA6 (1:20,000; Epitomics). The membranes were washed three times in TBST for 5 mins each and were incubated at room temperature for 1 hr with horseradish peroxidase conjugated rabbit anti-mouse or anti-rabbit IgG secondary antibody (Sigma-Aldrich, anti-mouse Cat. # A9044, anti-rabbit Cat. # A0545) diluted 1:10,000 in 1% TBST. Blots were subsequently washed three times with 1X TBST for 5 mins each and developed using a commercial chemiluminescent reagent (Clarity, Bio-Rad-170–5061) and imaged using the ChemiDoc MP (Bio-Rad). All incubation steps carried out at 4 °C or RT were done with gentle shaking. The quantification of blots was done by using Image Lab 5.0.

Statistical analysis. A summary of the number of samples used for the different experiments in these studies is shown in Supplemental Table 3.

For proteomics. Differentially expressed proteins were determined by applying Permutation Test with unadjusted significance level of $p < 0.05$ corrected by the Benjamini-Hochberg procedure to reduce the FDR ($p < 0.00674$ after using Benjamini-Hochberg procedure).

For western blotting and biological assays. Results are expressed as mean \pm standard deviation (SD) from at least three independent experiments. The comparisons between groups were performed using the Student's t-test or one-way ANOVA. P values of < 0.05 were defined as statistically significant.

Results

Proteomic profiling of male mice liver with quantitative 10-plex TMT LC-MS/MS showed significant differences between 7-day vehicle and ibuprofen treated mice livers. To our knowledge, this is the first report of proteomic profiling of mice liver treated with ibuprofen.

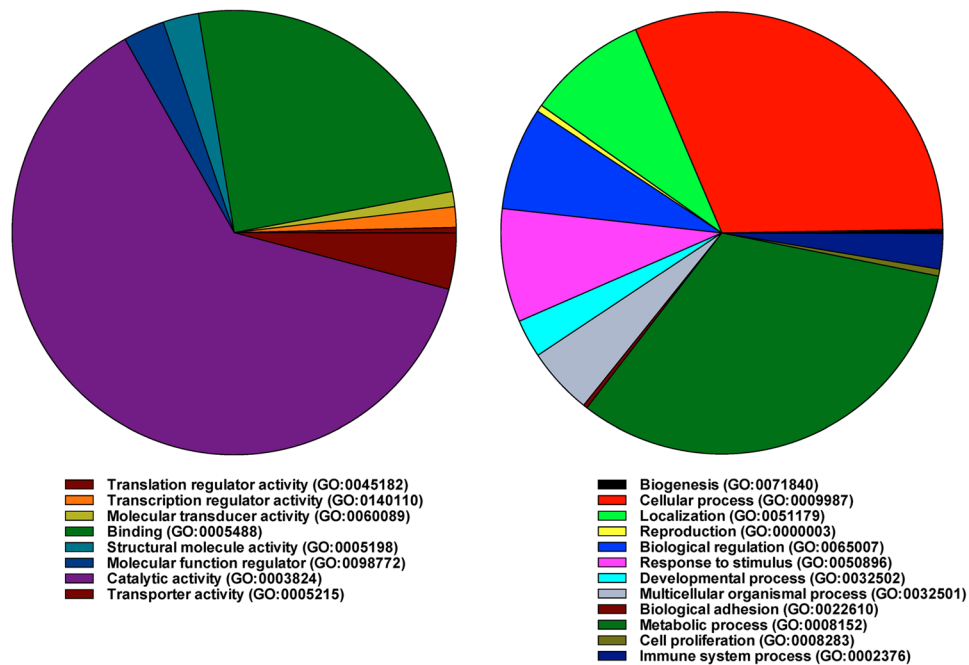


Figure 1. A pie chart depicting the proteomic analysis of control and ibuprofen-treated male mice liver. Biological processes associated with the differentially expressed proteins were shown using the PANTHER classification system.

Metabolic processes. The quantitative data obtained from mass spectrometry were analyzed using Panther program (<http://www.pantherdb.org/about.jsp>). The data revealed that when differentially expressed proteins were grouped by biological process, proteins associated with metabolic processes (GO:0008152) were the largest group of proteins that were altered (32.4%) in male ibuprofen-treated mice (Fig. 1). The other major biological process with the most proteins altered was cellular processes (GO:0009987) (Fig. 1). Based on molecular function, the comparison between the control and the ibuprofen treated mice livers showed that around 62.7% of the altered proteins were associated with catalytic activity (GO:0003824) (Fig. 1). Using the Panther Go-Slim program option, twenty-three biological processes showed a P-value of <0.001 and an FDR of $<0.5\%$ for over or under-represented differentially expressed proteins (Table 1). These processes included fatty acid, carbohydrate, steroid, coenzyme, acyl-CoA metabolic processes, respiratory electron transport chain, G protein-coupled receptor pathway, and cell surface receptor signaling.

Proteasome dysfunction. The proteomic data suggested that the level of the relatively low abundant proteasome subunit beta type-8 (PSMB8) ($\beta 5i$) was decreased in ibuprofen treated male mice (Supplemental Table 1). During stress conditions, the constitutive proteasome $\beta 1$, $\beta 2$ and $\beta 5$ subunits of 20S proteasome are replaced by $\beta 1i$, $\beta 2i$, and $\beta 5i$ immunoproteasome counterparts^{24–26}. Western blotting data showed that the expression levels of $\beta 5i$ immunoproteasome subunit was significantly decreased in ibuprofen treated male livers, consistent with the proteomic data (Fig. 2A,B). However, $\beta 5i$ was significantly increased in ibuprofen treated female livers relative to control (Fig. 2C). The $\beta 1i$ subunit expression was considerably elevated in ibuprofen treated female livers but not in males whereas no change was observed in the levels of $\beta 2i$ expression in both male and female livers (Fig. 2B,C). The expression levels of PSMA6 (20S catalytic core subunit) in the ibuprofen treated male livers was significantly elevated relative to controls whereas no change was observed in female mice livers treated with ibuprofen and controls (Fig. 2B,C). Since changes in proteasome activity are suggested to be associated with various pathological conditions including aging, cardiac and neurodegenerative diseases^{27–29}, we investigated the effects of ibuprofen on the proteasome and immunoproteasome activities. The $\beta 1$ (caspase-like) proteasome activity was significantly decreased in ibuprofen treated male livers while significantly increased in ibuprofen treated female livers compared to control animals (Fig. 2D,E). The $\beta 2$ (trypsin-like) activity was found to be significantly elevated in male livers, and equally significant (0.050) in ibuprofen-treated female livers relative to normal control livers (Fig. 2D,E). The $\beta 5$ (chymotrypsin-like) activity was significantly decreased in ibuprofen treated female livers and showed a trend toward decrease ($p = 0.085$) in ibuprofen treated male livers (Fig. 2D,E). No change in immunoproteasome activities was observed in ibuprofen treated male and female livers compared to normal control livers (Fig. 2F,G).

To further investigate if ibuprofen altered proteasome function enough to change the levels of the ubiquitinated and oxidized proteins, liver lysates were probed with anti-ubiquitin and anti-DNPH antibodies. The levels of polyubiquitinated and free ubiquitin proteins remained unchanged in both ibuprofen treated male and female livers (Fig. 3A,B). However, the levels of oxidized proteins decreased in ibuprofen treated male livers but not in ibuprofen-treated female livers (Fig. 3A).

| PANTHER GO-Slim Biological Process | Number of differentially expressed proteins | Expected | Fold Enrichment | +/- | Raw P value | False discover rate (FDR) |
|--|---|----------|-----------------|-----|-------------|---------------------------|
| fatty acid beta-oxidation | 7 | 0.25 | 27.56 | + | 2.93E-08 | 7.94E-07 |
| fatty acid metabolic process | 26 | 2.23 | 11.67 | + | 4.67E-19 | 3.80E-17 |
| lipid metabolic process | 44 | 5.21 | 8.45 | + | 1.94E-26 | 4.75E-24 |
| primary metabolic process | 98 | 55.86 | 1.75 | + | 3.18E-09 | 1.11E-07 |
| metabolic process | 125 | 69.37 | 1.8 | + | 2.29E-13 | 1.40E-11 |
| pentose-phosphate shunt | 2 | 0.08 | 24.75 | + | 4.43E-03 | 3.28E-02 |
| carbohydrate metabolic process | 12 | 3.6 | 3.33 | + | 3.73E-04 | 4.33E-03 |
| vitamin biosynthetic process | 3 | 0.13 | 23.62 | + | 4.87E-04 | 4.95E-03 |
| vitamin metabolic process | 3 | 0.25 | 11.81 | + | 2.81E-03 | 2.14E-02 |
| cellular amino acid biosynthetic process | 11 | 0.72 | 15.37 | + | 6.58E-10 | 2.68E-08 |
| cellular amino acid metabolic process | 31 | 2.62 | 11.83 | + | 1.07E-22 | 1.31E-20 |
| porphyrin-containing compound metabolic process | 3 | 0.24 | 12.37 | + | 2.49E-03 | 1.96E-02 |
| cellular amino acid catabolic process | 8 | 0.66 | 12.16 | + | 7.43E-07 | 1.81E-05 |
| acyl-CoA metabolic process | 5 | 0.43 | 11.71 | + | 1.12E-04 | 1.61E-03 |
| coenzyme metabolic process | 12 | 1.25 | 9.62 | + | 1.34E-08 | 4.08E-07 |
| cholesterol metabolic process | 4 | 0.42 | 9.62 | + | 1.10E-03 | 1.03E-02 |
| steroid metabolic process | 14 | 1.42 | 9.86 | + | 6.07E-10 | 2.96E-08 |
| lipid transport | 6 | 0.84 | 7.12 | + | 2.89E-04 | 3.71E-03 |
| respiratory electron transport chain | 8 | 1.29 | 6.19 | + | 7.21E-05 | 1.17E-03 |
| generation of precursor metabolites and energy | 10 | 2.11 | 4.73 | + | 7.90E-05 | 1.20E-03 |
| sulfur compound metabolic process | 5 | 0.88 | 5.7 | + | 2.36E-03 | 1.98E-02 |
| muscle contraction | 7 | 1.26 | 5.56 | + | 3.77E-04 | 4.18E-03 |
| phospholipid metabolic process | 7 | 2.05 | 3.41 | + | 5.48E-03 | 3.82E-02 |
| catabolic process | 33 | 13.9 | 2.37 | + | 5.62E-06 | 1.25E-04 |
| regulation of biological process | 16 | 38.33 | 0.42 | - | 2.77E-05 | 5.20E-04 |
| biological regulation | 25 | 45.01 | 0.56 | - | 6.55E-04 | 6.39E-03 |
| RNA metabolic process | 6 | 17.73 | 0.34 | - | 1.75E-03 | 1.53E-02 |
| nucleobase-containing compound metabolic process | 17 | 31.29 | 0.54 | - | 5.07E-03 | 3.64E-02 |
| G-protein coupled receptor signaling pathway | 0 | 10.1 | <0.01 | - | 6.12E-05 | 1.07E-03 |
| cell surface receptor signaling pathway | 4 | 19.96 | 0.2 | - | 2.65E-05 | 5.40E-04 |
| signal transduction | 17 | 33.43 | 0.51 | - | 1.41E-03 | 1.27E-02 |
| cell communication | 21 | 37.74 | 0.56 | - | 2.40E-03 | 1.95E-02 |
| sensory perception of smell | 0 | 8.07 | <0.01 | - | 4.54E-04 | 4.82E-03 |
| sensory perception of chemical stimulus | 0 | 8.64 | <0.01 | - | 3.09E-04 | 3.77E-03 |

Table 1. Biological processes in mice liver affected by ibuprofen treatment. Twenty-three biological processes showed a p value of <0.001 and an FDR of <0.5% for over or underrepresented differentially expressed proteins using the Panther program.

Energy production pathways. The proteomic data revealed that several proteins related to fatty acid metabolism and glycolytic pathway as well as other metabolic pathways were either upregulated or downregulated in ibuprofen treated male mice liver compared to control. To better understand the underlying molecular mechanisms, validation of the expression levels of different proteins associated with different energy metabolic pathways was carried out using Western blotting and biochemical assays to determine altered pathways activities.

Fatty acid metabolism pathway. To validate the expression levels of proteins related to β fatty acid metabolism the total liver lysates from male and female mice were probed with several antibodies to investigate the enzymes involved in fatty acid metabolism. The data suggests that all four proteins FAS (fatty acid synthase), LFABP (liver fatty acid-binding protein), CROT (carnitine O-octanoyltransferase), and FAAH (fatty acid amide hydrolase) (Fig. 4B) were significantly upregulated in male livers, consistent with proteomic data (Fig. 4A), whereas only FAS and LFABP was upregulated in ibuprofen treated female livers (Fig. 4C).

Since nearly all the enzymes involved in both mitochondrial β oxidation and peroxisomal β oxidation were upregulated by ibuprofen (Fig. 5, Supplemental Fig. 3), we measured H_2O_2 levels in the liver (Fig. 4E,G). H_2O_2 are reactive oxygen species that is increased when peroxisomal β oxidation is increased, and functions both as intracellular messenger and as a source of oxidative stress³⁰. In mice livers treated with ibuprofen, H_2O_2 was found to be significantly increased by 1.56-fold in male and 2.75-fold in females (Fig. 4E,G). Increases in H_2O_2 may lead to increases in catalase activity, and we observed significantly increased catalase activity in ibuprofen treated male livers (Fig. 4D) as well as in female mice livers (Fig. 4E).

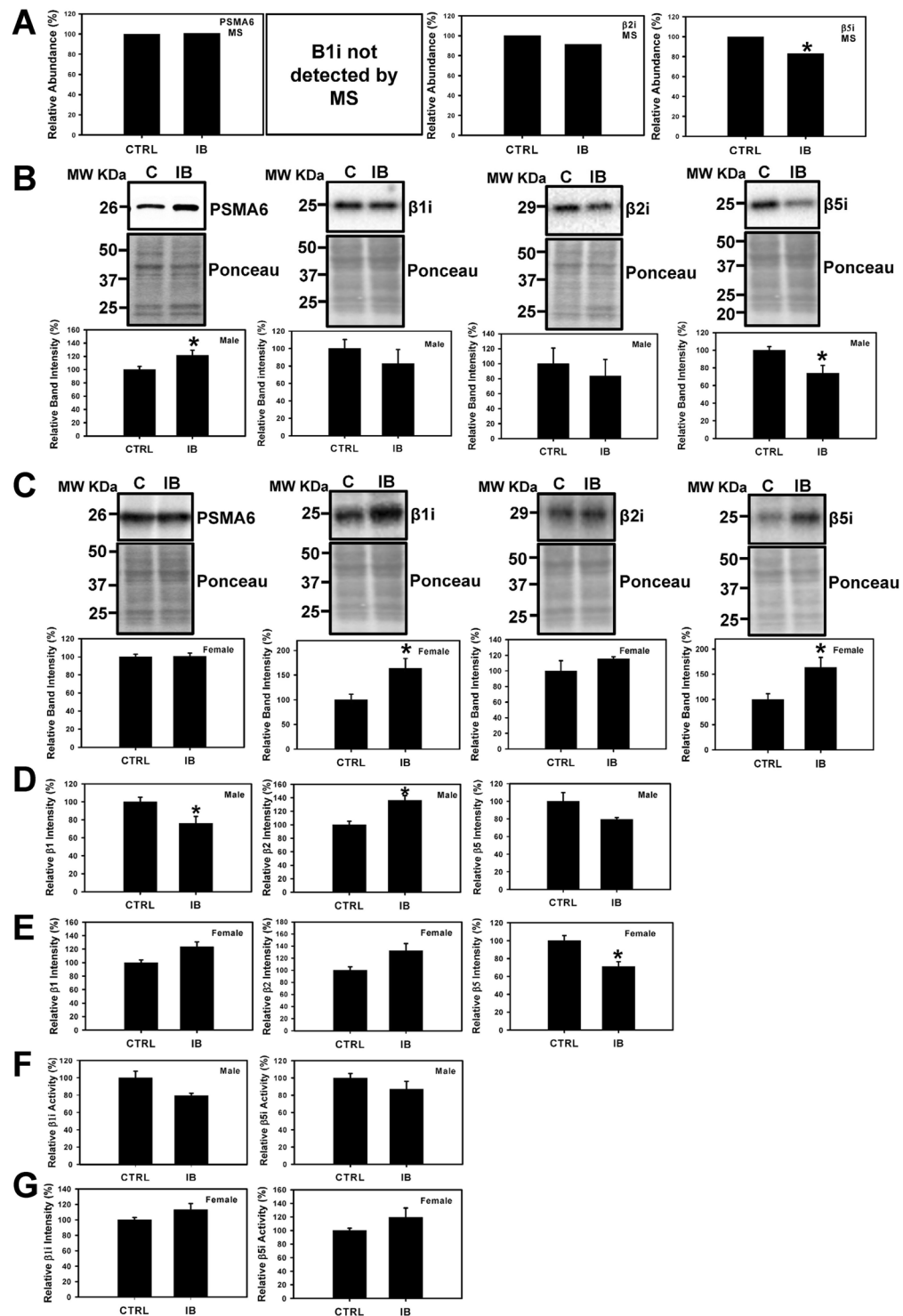


Figure 2. Effects of ibuprofen treatment on 20S proteasome and immuno-proteasome expression levels and activities in mice liver. (A) Changes in level of 26S proteasome subunits (β1, β2 and β5) and immunoproteasome subunits (β1i and β5i) obtained by mass spectrometry. Western blots of proteasome levels (PSMA6, β1i, β2i and β5i) and total protein (used as loading controls) in (B) Male liver, and (C) Female liver. Value are mean ± SE; n = 4–6 per group. *p < 0.05. (D) 26S proteasome (β1, β2 and β5) activities of liver lysates from male mice. (E) 26S proteasome (β1, β2 and β5) activities of liver lysates from female mice. (F,G) β1i and β5i immune-proteasome activities of male and female liver lysates. Value are mean ± SE; n = 6 per group. *p < 0.05.

Other enzymes involved in fat and drug metabolism. Since proteomic results showed that CYP4A10 (cytochrome P450 A10) and CYP4A14 increased by 1.74 and 3.03-fold in ibuprofen treated male livers and antibodies to these were unavailable, we determined the expression of CYP4A1 which has >90% sequence homology with CYP4A10.

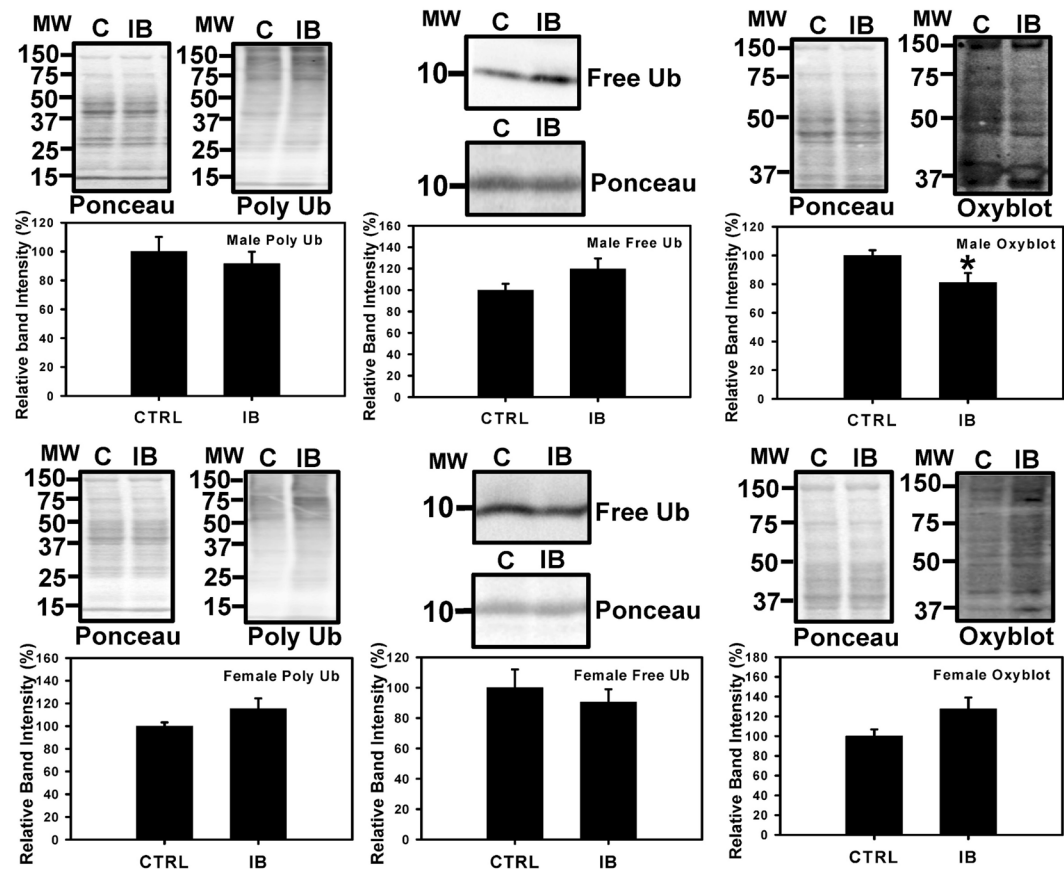


Figure 3. Characterization of levels of polyubiquitination, free ubiquitins and oxidized proteins in male and female mice livers. Western blot of polyubiquitinated, free ubiquitin levels and oxidized proteins in total liver lysates from mice (A) Male livers & (B) Female livers. Value are mean \pm SE; $n = 6$ per group. * $p < 0.05$.

The expression levels of CYP4A1 was significantly increased, 17 β -HSD2 (17 β hydroxyl steroid dehydrogenase type 2) was decreased, and CYP4A2 (cytochrome P450 1A2) not statistically changed in ibuprofen treated male livers (Fig. 6B). In contrast, the levels of CYP4A1 was decreased and CYP4A2 and 17 β -HSD2 were increased in female livers treated with ibuprofen (Fig. 6C), suggesting a gender-specific difference in mice liver. A summary of some of the data is shown in Fig. 5.

Glycolytic pathway. Validation of glycolytic pathway proteins using Western blotting showed that the expression levels of PKLR (pyruvate kinase, liver and RBC), and PFK-1 (Phosphofructokinases-1) was downregulated in male livers than controls (Fig. 6E) while levels of PKLR was upregulated in ibuprofen treated female livers suggesting a gender-specific difference with respect to glycolytic pathway. However, no difference was observed in the levels of PFK-1 in female livers (Fig. 6F).

Mitochondrial proteins. Consistent with proteomic data (Supplementary Fig. 2A) expression levels of inner mitochondrial membrane proteins Prohibitin-2 and ETFDH (electron transfer flavoprotein dehydrogenase) were both increased in male livers (Supplementary Fig. 2B). ATP5F1 (mitochondrial ATP synthase 5F1) showed a small increase in the proteomic studies but showed a decrease by Western blotting. The levels of ATP5F1, Prohibitin-2 and ETFDH were significantly increased in female livers treated with ibuprofen (Supplementary Figure 2C).

Antioxidant defense system. During oxidative stress and other stress conditions increased levels of H₂O₂ is associated with elevated production of antioxidant enzymes³¹. The proteomic data showed that various antioxidant enzymes such as glutathione S-transferase theta 2 (GSTT2), glutathione S-transferase Mu 1 (GSTM1), and glutathione S-transferase alpha 1/2/5 (GSTA1/2/5) were upregulated in male mice livers treated with ibuprofen compared to controls (Fig. 7A, Supplementary Table 1). To independently validate the results, the expression levels of GSTT2, GSTM1 and GSTA1/2/5 were analyzed by Western blotting. The expression of GSTM1 and GSTA1/2/5 was significantly upregulated in ibuprofen-treated male livers consistent with the proteomic data (Fig. 7B). In female ibuprofen-treated livers only the expression of GSTA1/2/5 was upregulated (Fig. 7C). Although not statistically significant, a trend towards increased GSTT2 (male) and GSTM1 (female) expression was observed in ibuprofen treated groups relative to control groups (Fig. 7B,C).

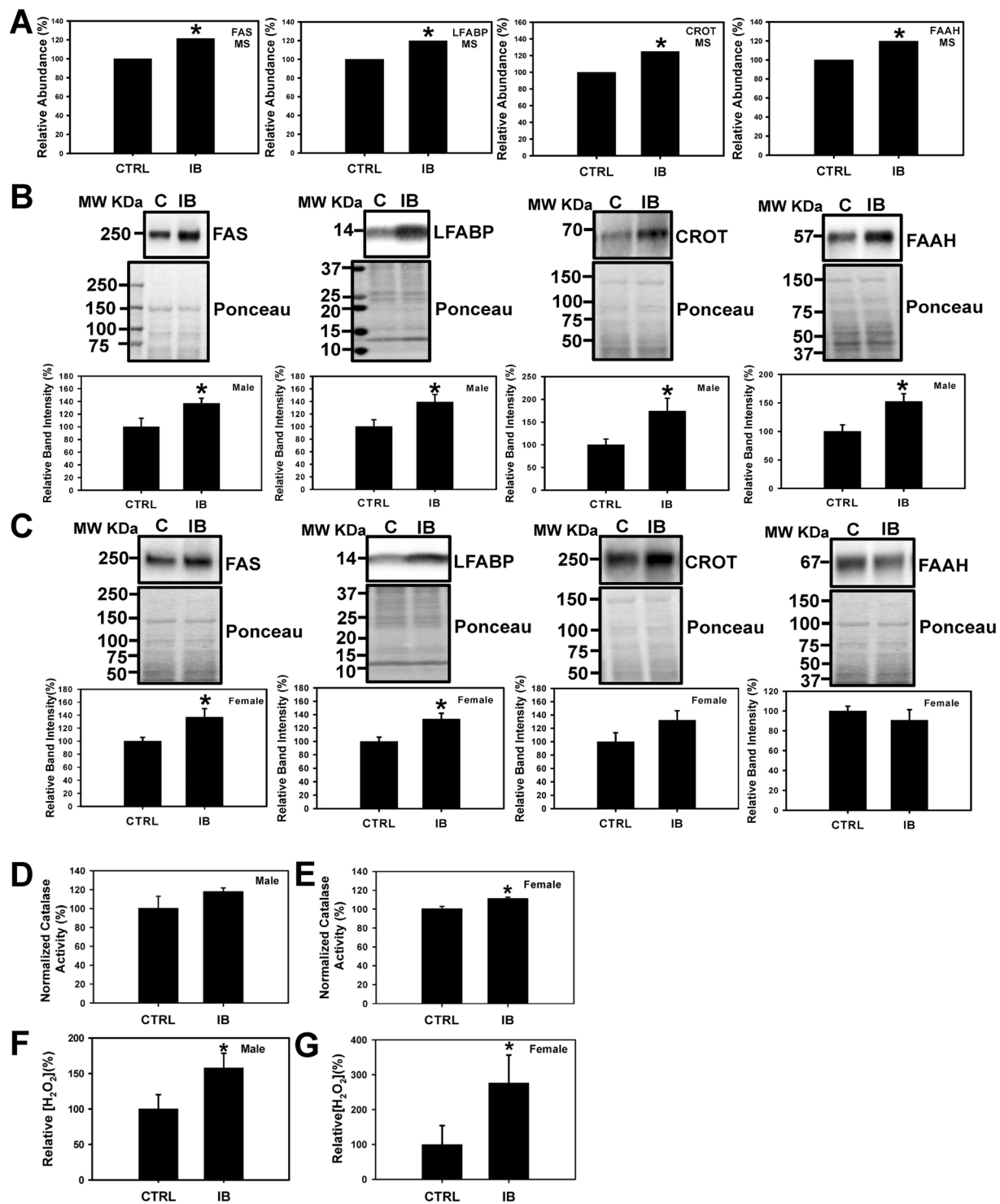


Figure 4. Validation of expression levels of proteins related to fatty acid metabolism pathway in male and female mouse liver. (A) Changes in the level of proteins FAS (Fatty Acid Synthase), LFABP (Liver Fatty acid-binding protein), CROT (carnitine O-octanoyltransferase), and FAAH (fatty acid amide hydrolase) obtained from mass spectrometry. Western blots and corresponding semi quantitative bar graphs for proteins, FAS, LFABP, CROT, and FAAH and total protein (used as a loading control) (B) Male liver and (C) Female liver. Value are mean \pm SE; $n = 4-6$ per group. * $p < 0.05$. Characterization of antioxidant catalase activity and hydrogen peroxide levels in control and ibuprofen-treated mouse livers. (D), (E) Catalase activity in male and female mouse liver. (F), (G) Relative hydrogen peroxide (H₂O₂) levels of male and female liver lysates. Value are mean \pm SE; $n = 5$ per group. * $p < 0.05$.

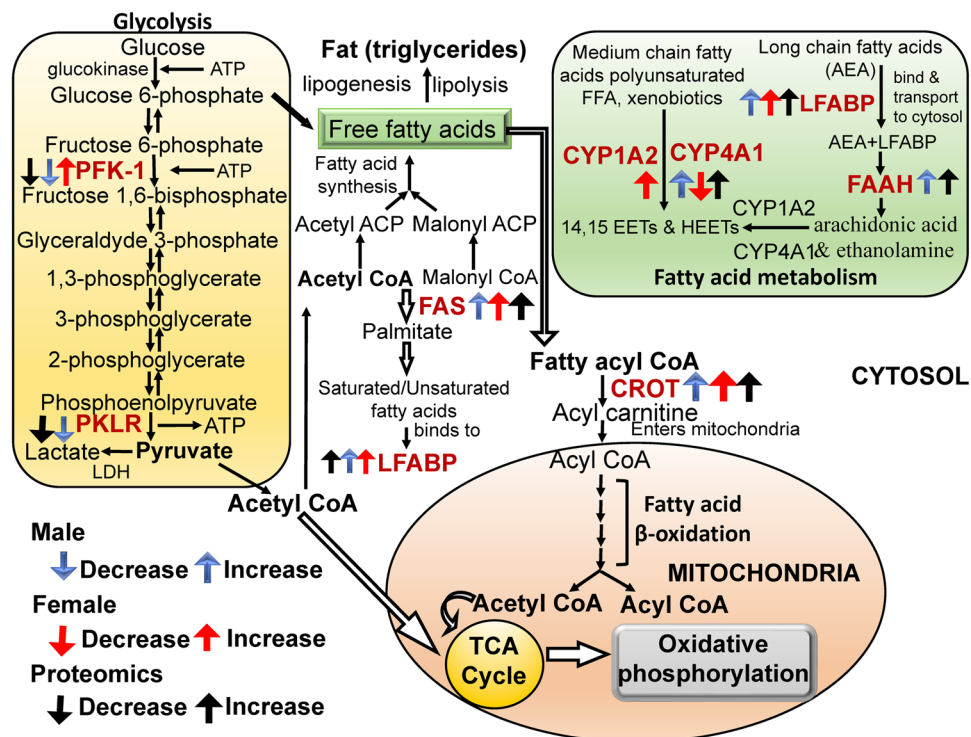


Figure 5. Schematic diagram showing the changes in the levels and expression of enzymes involved in the glycolytic and fatty acid pathways in ibuprofen treated male and female mice livers. Abbreviations: PFK-1 (Phosphofruktokinases-1); PKLR (pyruvate kinase, liver and RBC); FAS (Fatty acid synthase); LFABP (Liver Fatty acid-binding protein); FAAH (fatty acid amide hydrolase); CROT (carnitine O-octanoyltransferase); CYP4A1 (Cytochrome P450 4A1); ATP (Adenosine triphosphate); CYP1A2 (Cytochrome P450 1A2); TCA (tricarboxylic acid cycle).

Discussion

It is well acknowledged that high dose and long term use of NSAIDs are associated with adverse effects that include cardiac, gastrointestinal, renal and hepatotoxicity^{32,33}. The investigation of male mice liver using mass spectrometry suggests that even moderate dosages of ibuprofen treatment affect various critical cellular pathways. Since liver is a major player in metabolism, this approach also provides mechanistic quantitative information on the molecular pathways that are affected by drug toxicity³⁴. Various NSAIDs such as bromfenac, benoxaprofen and lumiracoxib were withdrawn from the market due to severe hepatotoxicity^{35,36}. The incidence rate of drug-induced liver injury in outpatients in France was found to be fourteen per 100000 patients³⁷. However, this is considered an underestimation as it will be unlikely to be detected in smaller clinical trials, and a more recent study in 2010 found that NSAIDs including ibuprofen (odds ratio of 2.24, 95% confidence interval (CI) = 1.99–2.52) increased the risk of hospitalization due to acute hepatitis (odds ratio 2.13, 95% CI = 2–2.18)³⁵. The frequency of drug-related hepatic injuries, including from NSAIDs, was found to be different in Spain and France suggesting that several factors besides the NSAIDs, such as drug use patterns and/or genetic and environmental factors, may be important³⁶.

Upadhyay *et al.*, showed that ibuprofen induced proteasome dysfunction, mitochondrial-mediated apoptosis, and cell death in A549 and/or Cos-7 cells³⁸. However, the cell death, proteasome inhibition and apoptosis were observed using 1 mM ibuprofen, which is significantly higher than the peak ibuprofen concentrations found in human blood (58.4 µg/mL or 283.09 µM) after high doses of ibuprofen³⁹, and as such may not be physiologically relevant. The proteomic results suggested that the immunoproteasome subunit β5i was decreased in livers from ibuprofen treated male mice and Western blotting and proteasome assays suggest gender-specific differences with respect to proteasome and immunoproteasome activities. The proteasome is part of the ubiquitin proteasome system (UPS), which is critical for protein quality control and is the main intracellular degradation pathway that eliminates polyubiquitinated misfolded and oxidized proteins by a multi-complex 26 S proteasome^{16,17,24,40}. The 26S mainly degrades polyubiquitinated proteins in an ATP dependent manner and contains caspase-like, trypsin-like and chymotrypsin-like proteolytically active sites in the β1 (PSMB6), β2 (PSMB7), and β5 (PSMB5) subunits of the 20S core^{24,41}. On induction with interferon-γ (IFN-γ), the constitutive β1, β2 and β5 subunits of 20S proteasome are replaced by catalytically active inducible β1i (PSMB9), β2i (PSMB10) and β5i (PSMB8) subunits referred as the immunoproteasome^{24,25}. The immunoproteasome plays an important role in degrading oxidized proteins, preventing protein aggregation, cytokine production, antigen presentation and T cell differentiation, and survival^{24,42}.

The expression of the immunoproteasome β5i, which is important for the degradation of oxidized proteins under stressful conditions, was decreased in ibuprofen treated male livers relative to controls whereas it was

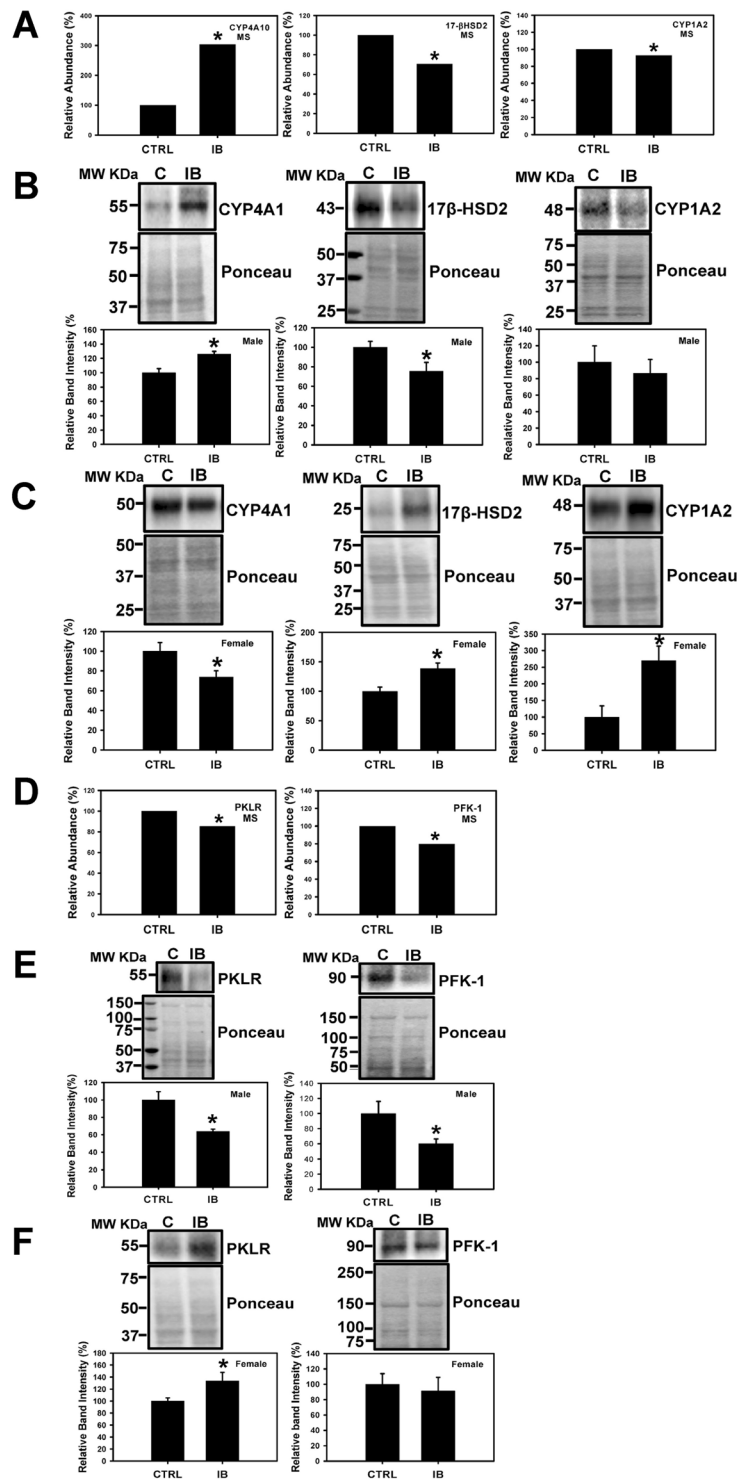


Figure 6. Determination and validation of expression levels of proteins related to fatty acid metabolism and glycolytic pathways in mouse liver. Changes in level of CYP4A10 (Cytochrome P450 4A10), 17β-HSD2 (17β hydroxysteroid dehydrogenase type 2), and CYP1A2 (Cytochrome P450 1A2) obtained by mass spectrometry (A). Western blots and corresponding semi quantitative bar graphs for CYP4A1, 17β-HSD2, and CYP1A2 (Cytochrome P450 1A2) and total protein (used as a loading control). (B) Male liver and (C) Female liver. Value are mean ± SE; n = 4–6 per group. *p < 0.05. (D) Proteomic analysis and Western blots of proteins, PKLR (pyruvate kinase, liver and RBC), and PFK-1 (Phosphofructokinases-1), total protein (used as a loading control) and corresponding semi- quantitative bar graphs are shown for (E) male mice liver, and (F) female mice liver. Value are mean ± SE; n = 4–6 per group. *p < 0.05.

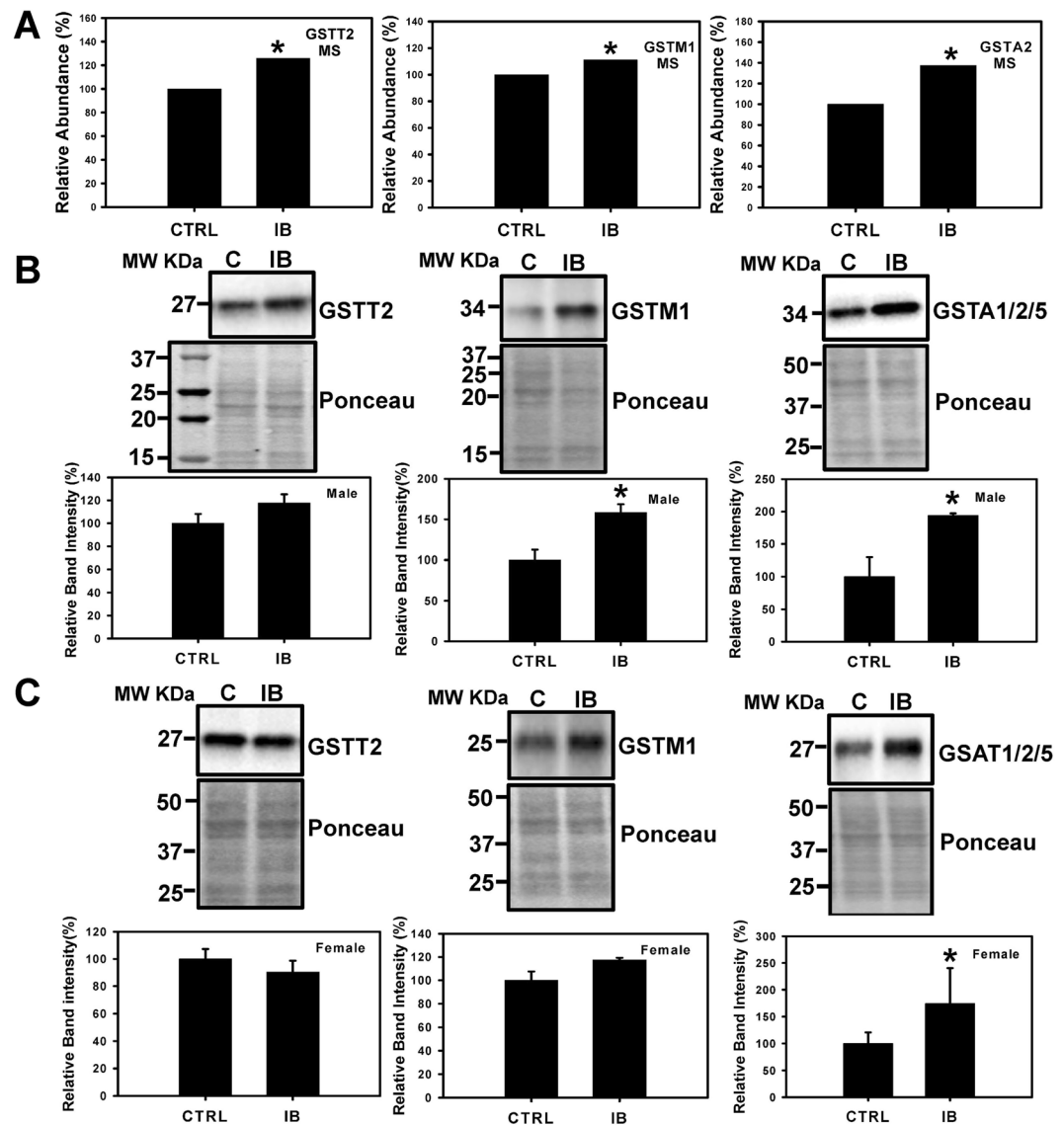


Figure 7. Effect of short-term ibuprofen treatment (7 days) on levels of oxidative-stress related proteins in control and ibuprofen-treated mouse livers. Change in levels of protein associated with oxidative stress, GSTT2 (Glutathione S-transferase theta-2), GSTMI (Glutathione S-transferase mu 1), and GSTA1/2/5 (Glutathione S-transferase alpha 1/2/5) obtained by mass spectrometry (A). Western blot analysis was performed to determine the expression levels of protein associated with oxidative stress, GSTT2, GSTMI, and GSTA1/2/5 in (B) Male mouse livers, and (C) Female mouse livers. Band signal intensities were analyzed by Image Lab® Software Version 12 and normalized with intensities obtained from loading control after staining with commercial Ponceau S for total protein. Value are mean \pm SE; $n = 4-6$ per group. * $p < 0.05$.

increased in female mice livers in ibuprofen treated group. Despite the decrease in $\beta 5i$ expression in male livers and increased expression of $\beta 5i$ and $\beta 1i$ in female livers, the 26S $\beta 5i$ and $\beta 1i$ immunoproteasome activities remain unchanged in both ibuprofen treated male and female livers. Altered proteasome function is typically associated with increased levels of oxidized proteins and these possibilities were investigated in both male and female livers. The levels of oxidized proteins decreased in ibuprofen treated male livers compared to controls, while not significant, a trend towards the increase in levels of oxidized proteins ($P = 0.086$) was observed in ibuprofen-treated female livers relative to controls. A substantial decrease in $\beta 1$ proteasome activity and $\beta 5i$ expression suggest altered proteasome functions in male livers. The elevated expression of 20S proteasome (increased PSMA6), which play an important role in the elimination of oxidized proteins, might be one of the mechanisms that account for reduced levels of oxidized proteins in male livers. However, in female livers increased $\beta 1$, $\beta 1i$ and $\beta 5i$ expression, as well as a trend towards the increase in proteasome activities ($\beta 2$, $\beta 1i$, $\beta 5i$) and $\beta 2i$ expression, suggest that ibuprofen activated a compensated stress response in female livers as a mechanism to adapt to various stressors. It has been previously documented that increased oxidative stress regulates proteasome and immunoproteasome functions⁴³. Altogether these results suggest that ibuprofen causes proteasome dysfunction in both mice genders, male mice respond differently than female mice with respect to proteasome function.

Proteins involved in antioxidant defense system. Mass spectrometry data showed that various antioxidant enzymes such as GSTT2, GSTM1 and GSTA1/2/5 that helps to eliminate toxic metabolites generated by oxidative stress were upregulated in response to ibuprofen treatment in male mice livers than controls. The expression levels of GSTM1 and GSTA1/2/5 (significant) was higher in ibuprofen-treated male livers. Similarly, in female ibuprofen-treated livers the expression of GSTA1/2/5 was upregulated significantly. GSTT2 (male) and GSTM1 (female) showed a trend toward higher levels relative to respective controls. Catalase activity, an important antioxidant activity, showed higher levels in both male and female livers. Increased levels of H₂O₂ was observed in both ibuprofen treated male and female livers relative to controls. During oxidative stress and other stress, conditions increased levels of H₂O₂ is associated with elevated production of antioxidant enzymes as a defense mechanism³¹ that explains the upregulation of anti-oxidant pathways in both male and female livers treated with ibuprofen. Also, the glutathione system plays regulatory role to maintain redox state of the cell⁴⁴.

Proteins involved in energy metabolism. Mass spectrometry showed that proteins associated with metabolic processes are the largest group of differentially expressed proteins that occur in response to ibuprofen treatment in male livers relative to controls. Western blotting showed that two of the three key enzymes involved in regulating glycolysis, pyruvate kinase L/R-type (PKLR) and phosphofructokinase 1 (PFK-1), were downregulated in male livers compared to controls. In contrast, PKLR was upregulated while no difference in the levels of PFK-1 was observed in ibuprofen treated female livers. PKLR is an enzyme responsible for catalyzing the conversion of phosphoenolpyruvate and adenosine triphosphate (ATP) to pyruvate and ATP in glycolysis⁴⁵. PFK catalyzes the rate-limiting phosphorylation of fructose-6-phosphate to fructose-1,6-diphosphate. Downregulation or deficiency of pyruvate kinase leads to ATP depletion which in turn affects cell viability as well as accumulation of the glycolytic intermediates (2,3-diphosphoglycerate (2,3-DPG) that eventually leads to impaired glycolytic flux⁴⁶. In isolated perfused rat livers mefenamic acid was reported to stimulate glycolysis, oxygen uptake, glycogenolysis and fructolysis⁴⁷. PFK null mice were characterized by reduced lifespan, exercise intolerance and progressive cardiac hypertrophy⁴⁸. Thus, the lower expression of PKLR and PFK-1 suggest that the ibuprofen affects metabolism and altered hepatic glucose metabolism in male mice. The upregulation of PKLR in female livers suggests accelerated glycolysis as an adaptive response to compensate for the depletion of ATP against oxidative stress.

Differential changes in PKLR in males (decreased) and females (increased) could have significant functional consequences in liver since glycolytic inhibition (such as by decreases in PKM2) has been suggested to promote the pentose phosphate pathway to generate higher levels of NADPH. NADPH is important in recycling oxidized glutathione and provides the reducing power needed for protein-based antioxidant systems⁴⁹. ATP5F1 is part of the ATP synthase complex which generates ATP. ATP5F1 was reduced in male mice and increased in female mice compared to controls. In some cell types reduced ATP levels have been found to promote oxidative stress⁵⁰. The electron transport chain is also a major site for superoxide production⁵¹. These results support several publications which suggest that oxidative stress is higher in male rats than female rats^{52,53}.

A deficiency in cellular ATP has been suggested to cause several diseases⁵⁴. In a mouse model of Leigh syndrome caused by a deficiency in a component of complex I, the levels of ATP were observed to dictate disease severity and neuronal death⁵⁵. Intracellular ATP concentrations have also been shown to be important in intracellular protein degradation with the proteasomal activity being regulated by ATP levels⁵⁶. Importantly, impaired bioenergetics affects the redox balance of a cell⁵⁷. ROS can also induce bioenergetic changes in cells and tissues, such as in liver where ROS induced changes in glucose and lipid metabolism⁵⁸.

The mass spectrometry data also suggest that other metabolic pathways are affected, and these include pathways previously reported and summarized by Porter *et al.*⁵⁹, such as the pentose phosphate shunt and the electron transport chain. Evidence for NSAIDs altering other pathways such as cholesterol⁶⁰, and vitamin⁶¹ metabolic pathways all support the proteomic data. Other pathways that were found to be affected by NSAIDs that were not previously reported include steroid, phospholipid, sulfur compound, and amino acid metabolic pathways.

Proteins involved in fatty acid metabolism. *Proteins involved in fatty acid biosynthesis.* Glucose and fatty acids are metabolized in the liver and regulate whole-body energy homeostasis⁷. At high glucose levels, glycolysis is dominant and glycolytic intermediates and products are utilized to generate ATP as well as lipids and amino acids. During energy deprivation (low glucose levels), hepatocytes switch from glycolysis to fatty acid β oxidation for energy production⁷. Fatty acid oxidation depends upon the plasma concentration of free fatty acids and occurs in three subcellular organelles, the mitochondria and peroxisomes which carried out β -oxidation, whereas ω -oxidation catalyzed by CYP4A1 takes place in endoplasmic reticulum⁶². FAS is an important enzyme of fatty acid biosynthesis which in the presence of NADPH catalyzes the condensation of acetyl-CoA and malonyl-CoA to generate palmitic acid⁶³. In normal healthy tissues, FAS is expressed at very low levels. High expression of FAS is correlated with molecular changes in various types of cancer cells including breast cancer^{64–66}. Ibuprofen treatment stimulated higher expression of FAS in both male and female livers suggesting altered fatty acid metabolism.

Proteins involved in fatty acid oxidation. In liver, fatty acids are metabolized by two major metabolic pathways; they either undergo β -oxidation in mitochondria and peroxisomes to produce ATP for energy requirements or esterified to triglycerides to generate either lipoproteins to export or lipid droplets for storage. The short, medium and long fatty acid chains are oxidized in mitochondria whereas very long chain fatty acids are degraded by peroxisomes⁶⁷. Kasuya *et al.* reported that various NSAIDs (diflunisal, enoxacin, salicylic acid, aspirin and ofloxacin) and quinolone antimicrobial drugs have inhibitory effects on the medium chain acyl-CoA synthetase in mouse and bovine liver mitochondria⁶⁸. LFABP regulates the lipid β -oxidation in mammalian liver and intestine and is correlated with various disease conditions including obesity, type 2 diabetes, insulin resistance, and fatty

liver disease in humans^{69,70}. Elevated expression of LFABP in ibuprofen treated male and female livers together with increased levels of H₂O₂ (a byproduct of fatty acid β -oxidation) is indicative of increased fatty acid metabolism. FAAH is a membrane-bound enzyme that plays an important role in breaking endogenous fatty acid amides such as the endogenous cannabimimetic agent anandamide (AEA) and palmitoylethanolamide (PEA) (an anti-inflammatory agent)⁷¹. NSAIDs such as aspirin, ibuprofen, and indomethacin were reported to have inhibitory action on FAAH with different potencies. Ibuprofen was shown to attenuate the metabolism of AEA by FAAH in rat brain⁷¹. In this study ibuprofen significantly enhanced FAAH expression in male livers while no significant change in female livers was observed. Hence, gender-specific differences in fatty acid metabolism were observed in ibuprofen treated mice.

The CYP4A1 and 4A2 gene expression have been reported to increase with NSAIDs^{72–74}. CYP1-4 enzymes play an important role in the oxidative metabolism of fatty acids, steroids, polycyclic aromatic hydrocarbons (PAHs), various drugs such as acetaminophen, caffeine, clozapine, phenacetin, clomipramine and naproxen, and other carcinogens and environmental pollutants^{73,74}. When treated with ibuprofen male livers showed no change in CYP1A2 and elevated levels of CYP4A1 while female livers showed significantly elevated expression of CYP1A2 and lower expression of CYP4A1. The opposite effects of ibuprofen on CYP4A1 in male and female mice support previous publications which suggest that sex related differences occur with respect to drug metabolism and adverse reactions. Females have been shown to give a 1.5- to 1.7-fold higher risk factor for having adverse drug reactions than men⁷⁵. Although the underlying mechanism for these gender effects is not known, some of the differences have been attributed to the levels of sex hormones and their receptors⁷⁶. However, some studies suggest that estrous variability is no greater in females than the intrinsic variability in males⁷⁷. Some of the sex differences has also been linked to the expression of genes encoded by the X chromosome⁷⁸. Other data also suggest that sex differences could occur at specific ages and in certain environments⁷⁹. As such, we cannot assume that the sex related differences observed in this study is similar to what occurs at other ages. In these current studies, the sex-related differences observed may be partly due to sex-related differences in drug-metabolizing enzymes and drug transporters. The difference in the levels of CYP enzymes may also be related to the specific function of individual P450 enzymes and substrate specificity⁷³. Moreover, oxidative stress and inflammatory factors can modulate CYPs transcription⁸⁰. The increased oxidative stress in males could explain the lower expression of CYP4A1 in response to ibuprofen treatment. Although differential sex-related gene or protein expression of CYP4A1 has not been previously reported, many CYPs including CYP7A1 and CYP1B1 have been reported to show sex-related gene expression patterns^{81,82}.

CROT is a carnitine acyltransferase that plays crucial roles in lipid metabolism and fatty acid β -oxidation^{83,84}. Although localized to peroxisomes, CROT is essential for transport of medium and long length acyl-CoA chains from peroxisomes to the cytosol and mitochondria for further degradation⁸³. The high expression of CROT in male (statistically significant) and female (trend to increase) livers suggest that it is possible that ibuprofen treatment induces peroxisomal oxidation of medium and long chain fatty acids metabolism as a compensatory mechanism due to an overload of β -oxidation of fatty acids in mitochondria.

Other pathways proteins. 17 β -HSD2 is a microsomal enzyme that catalyzes the oxidation of sex steroids testosterone and estradiol (E2) to less active ketones androstenedione and estrone (E1)^{85,86}. It is reported that the inhibition of 17 β -HSD2 in a *in vivo* monkey model and osteoporosis patients is beneficial to increase in E2 and testosterone levels that facilitate reduction in bone resorption and maintenance of bone formation⁸⁷. The gender-specific effect of ibuprofen in our study suggests that ibuprofen has more pronounced effect on female livers as higher 17 β -HSD2 expression indicate more accumulation of sex hormone in females that will eventually lead to perturbed energy metabolism pathways. The age and sexual maturity of the mice used may also be important in the levels of the enzymes involved in sex hormone biosynthesis and may be partly responsible for some of the observed gender specific differences.

Limitations of the study. Our study observed gender-specific ibuprofen-mediated effects on mice liver. However, since the proteomic profiling was only done on male mice, the liver proteins and pathways investigated by Western blotting and biochemical assays were limited only to proteins which were identified as differentially regulated in liver of male mice. It is likely that female-specific changes in protein expression also occur in ibuprofen treated livers and these changes were not investigated. The effects observed may also be age specific and could be significantly different in mice of different ages.

Conclusion

Mass spectrometry showed that moderate levels of ibuprofen given to healthy mice for seven days resulted in over 300 proteins that were significantly altered when compared to control groups. Western blotting and biological assays showed that livers from male and female mice showed differences in the UPS, glycolysis and fatty acid metabolism. It is likely that many of the other pathways that were affected by ibuprofen also show gender differences, but these pathways were not investigated in this study. The data also suggests that ibuprofen affects previously unknown pathways such as amino acid, steroid and vitamin metabolism. Overall, our data indicate that moderate doses of ibuprofen can affect liver more significantly than previously reported and include proteasome dysfunction, increased levels of H₂O₂, impaired glycolytic pathways and altered fatty acid synthesis and oxidation. Although we expected similar differences between males and females with respect to ibuprofen treatment, complex gender-specific ibuprofen-mediated effects were observed. These gender-specific effects may be important for the side effects of ibuprofen (such as increased risk of stroke) and more research is needed to investigate this possibility. The amounts of ibuprofen taken by males and females may need to be altered in the future. Although the published experimental data to support that males and females show important physiological differences that

affect the pathophysiology of many common diseases is increasing at a steady pace, very little gender-specific health care is utilized worldwide. Ultimately, gender should be considered in drug use, as the toxicity of some drugs is significantly different between women and men.

Data availability

Raw data, and Scaffold results are available from the MassIVE proteomics repository (MSV000083987) and Proteome Exchange PXD014279. All Western Blot raw data generated or analyzed during this study are included in this published article (Supplementary Figure 4). The datasets generated during the current study are available from the corresponding author on reasonable request.

Received: 7 November 2019; Accepted: 3 February 2020;

Published online: 25 February 2020

References

- Irvine, J., Afrose, A. & Islam, N. Formulation and delivery strategies of ibuprofen: challenges and opportunities. *Drug. Dev. Ind. Pharm.* **44**, 173–183, <https://doi.org/10.1080/03639045.2017.1391838> (2018).
- Dill, J. *et al.* A molecular mechanism for ibuprofen-mediated RhoA inhibition in neurons. *J. neuroscience: Off. J. Soc. Neurosci.* **30**, 963–972, <https://doi.org/10.1523/JNEUROSCI.5045-09.2010> (2010).
- Rainsford, K. D. Ibuprofen: pharmacology, efficacy and safety. *Inflammopharmacology* **17**, 275–342, <https://doi.org/10.1007/s10787-009-0016-x> (2009).
- Smyth, E. M., Grosser, T., Wang, M., Yu, Y. & FitzGerald, G. A. Prostanoids in health and disease. *J. lipid Res.* **50**(Suppl), S423–428, <https://doi.org/10.1194/jlr.R800094-JLR200> (2009).
- Chang, S. Y. *et al.* Confirmation that cytochrome P450 2C8 (CYP2C8) plays a minor role in (S)-(+)- and (R)-(-)-ibuprofen hydroxylation *in vitro*. *Drug. Metab. disposition: Biol. fate Chem.* **36**, 2513–2522, <https://doi.org/10.1124/dmd.108.022970> (2008).
- Mazaleuskaya, L. L. *et al.* PharmGKB summary: ibuprofen pathways. *Pharmacogenetics genomics* **25**, 96–106, <https://doi.org/10.1097/FPC.000000000000113> (2015).
- Rui, L. Energy metabolism in the liver. *Compr. Physiol.* **4**, 177–197, <https://doi.org/10.1002/cphy.c130024> (2014).
- Gao, Y. *et al.* Proteomic analysis of acetaminophen-induced hepatotoxicity and identification of heme oxygenase 1 as a potential plasma biomarker of liver injury. *Proteomics. Clinical applications* **11**, <https://doi.org/10.1002/prca.201600123> (2017).
- Ghosh, R., Alajbegovic, A. & Gomes, A. V. NSAIDs and Cardiovascular Diseases: Role of Reactive Oxygen Species. *Oxid. Med. Cell. Longev.* **2015**, 536962, <https://doi.org/10.1155/2015/536962> (2015).
- Laster, J. & Satoskar, R. Aspirin-Induced Acute Liver. *Injury. ACG case Rep. J.* **2**, 48–49, <https://doi.org/10.14309/crj.2014.81> (2014).
- Wen, C. *et al.* Metabolism of liver CYP450 and ultrastructural changes after long-term administration of aspirin and ibuprofen. *Biomedicine pharmacotherapy=Biomedicine pharmacotherapie* **108**, 208–215, <https://doi.org/10.1016/j.biopha.2018.08.162> (2018).
- Ghosh, R., Hwang, S. M., Cui, Z., Gilda, J. E. & Gomes, A. V. Different effects of the nonsteroidal anti-inflammatory drugs meclofenamate sodium and naproxen sodium on proteasome activity in cardiac cells. *J. Mol. Cell Cardiol.* **94**, 131–144, <https://doi.org/10.1016/j.yjmcc.2016.03.016> (2016).
- Ghosh, R., Goswami, S. K., Feitoza, L., Hammock, B. & Gomes, A. V. Diclofenac induces proteasome and mitochondrial dysfunction in murine cardiomyocytes and hearts. *Int. J. Cardiol.* **223**, 923–935, <https://doi.org/10.1016/j.ijcard.2016.08.233> (2016).
- Jamil, A., Mahboob, A. & Ahmed, T. Ibuprofen targets neuronal pentraxins expression and improves cognitive function in mouse model of AlCl₃-induced neurotoxicity. *Exp. Ther. Med.* **11**, 601–606, <https://doi.org/10.1016/j.etm.2015.2928> (2016).
- Bendele, A. M., Hulman, J. F., White, S., Brodhecker, C. & Bendele, R. A. Hepatocellular proliferation in ibuprofen-treated mice. *Toxicol. Pathol.* **21**, 15–20, <https://doi.org/10.1177/019262339302100102> (1993).
- Reagan-Shaw, S., Nihal, M. & Ahmad, N. Dose translation from animal to human studies revisited. *FASEB J.* **22**, 659–661, <https://doi.org/10.1096/fj.07-9574LSF> (2008).
- Klotz, C., O'Flaherty, S., Goh, Y. J. & Barrangou, R. Investigating the Effect of Growth Phase on the Surface-Layer Associated Proteome of *Lactobacillus acidophilus* Using Quantitative Proteomics. *Front. Microbiol.* **8**, 2174, <https://doi.org/10.3389/fmicb.2017.02174> (2017).
- Rauniar, N. & Yates, J. R. III Isobaric labeling-based relative quantification in shotgun proteomics. *J. Proteome Res.* **13**, 5293–5309, <https://doi.org/10.1021/pr500880b> (2014).
- Ow, S. Y. *et al.* iTRAQ underestimation in simple and complex mixtures: “the good, the bad and the ugly”. *J. Proteome Res.* **8**, 5347–5355, <https://doi.org/10.1021/pr900634c> (2009).
- Gomes, A. V. *et al.* Proteomic analysis of physiological versus pathological cardiac remodeling in animal models expressing mutations in myosin essential light chains. *J. Muscle Res. Cell Motil.* **36**, 447–461, <https://doi.org/10.1007/s10974-015-9434-0> (2015).
- Shadforth, I. P., Dunkley, T. P., Lilley, K. S. & Bessant, C. i-Tracker: for quantitative proteomics using iTRAQ. *BMC Genomics* **6**, 145, <https://doi.org/10.1186/1471-2164-6-145> (2005).
- Oberg, A. L. *et al.* Statistical analysis of relative labeled mass spectrometry data from complex samples using ANOVA. *J. Proteome Res.* **7**, 225–233, <https://doi.org/10.1021/pr700734f> (2008).
- Cui, Z., Gilda, J. E. & Gomes, A. V. Crude and purified proteasome activity assays are affected by type of microplate. *Anal. Biochem.* **446**, 44–52, <https://doi.org/10.1016/j.ab.2013.10.018> (2014).
- Cui, Z., Hwang, S. M. & Gomes, A. V. Identification of the immunoproteasome as a novel regulator of skeletal muscle differentiation. *Mol. Cell. Biol.* **34**, 96–109, <https://doi.org/10.1128/MCB.00622-13> (2014).
- Kimura, H., Caturegli, P., Takahashi, M. & Suzuki, K. New Insights into the Function of the Immunoproteasome in Immune and Nonimmune Cells. *J. Immunology Res.* **2015**, 541984, <https://doi.org/10.1155/2015/541984> (2015).
- Cloos, J. *et al.* Immunoproteasomes as therapeutic target in acute leukemia. *Cancer Metastasis Rev.* **36**, 599–615, <https://doi.org/10.1007/s10555-017-9699-4> (2017).
- Collins, G. A. & Goldberg, A. L. The Logic of the 26S Proteasome. *Cell* **169**, 792–806, <https://doi.org/10.1016/j.cell.2017.04.023> (2017).
- Dantuma, N. P. & Bott, L. C. The ubiquitin-proteasome system in neurodegenerative diseases: precipitating factor, yet part of the solution. *Front. Mol. Neurosci.* **7**, 70, <https://doi.org/10.3389/fnmol.2014.00070> (2014).
- Ranek, M. J., Terpstra, E. J., Li, J., Kass, D. A. & Wang, X. Protein kinase g positively regulates proteasome-mediated degradation of misfolded proteins. *Circulation* **128**, 365–376, <https://doi.org/10.1161/CIRCULATIONAHA.113.001971> (2013).
- Wong, H. S., Dighe, P. A., Mezera, V., Monternier, P. A. & Brand, M. D. Production of superoxide and hydrogen peroxide from specific mitochondrial sites under different bioenergetic conditions. *J. Biol. Chem.* **292**, 16804–16809, <https://doi.org/10.1074/jbc.R117.789271> (2017).
- Veal, E. A., Day, A. M. & Morgan, B. A. Hydrogen peroxide sensing and signaling. *Mol. Cell* **26**, 1–14, <https://doi.org/10.1016/j.molcel.2007.03.016> (2007).

32. Scarim, C., de Oliveira Vizioli, E., Santos, J. & Chung, M. *NSAIDs and Natural Products Interactions: Mechanism and Clinical Implications*. (2017).
33. Fong, S. Y., Efferth, T. H. & Zuo, Z. Modulation of the pharmacokinetics, therapeutic and adverse effects of NSAIDs by Chinese herbal medicines. *Expert. Opin. Drug. Metab. Toxicol.* **10**, 1711–1739, <https://doi.org/10.1517/17425255.2014.970167> (2014).
34. Stamper, B. D., Mohar, L., Kavanagh, T. J. & Nelson, S. D. Proteomic analysis of acetaminophen-induced changes in mitochondrial protein expression using spectral counting. *Chem. Res. Toxicol.* **24**, 549–558, <https://doi.org/10.1021/tx1004198> (2011).
35. Lee, C. H., Wang, J. D. & Chen, P. C. Increased risk of hospitalization for acute hepatitis in patients with previous exposure to NSAIDs. *Pharmacoepidemiol. Drug. Saf.* **19**, 708–714, <https://doi.org/10.1002/pds.1966> (2010).
36. Lapeyre-Mestre, M. *et al.* Non-steroidal anti-inflammatory drug-related hepatic damage in France and Spain: analysis from national spontaneous reporting systems. *Fundam. Clin. Pharmacol.* **20**, 391–395, <https://doi.org/10.1111/j.1472-8206.2006.00416.x> (2006).
37. Sgro, C. *et al.* Incidence of drug-induced hepatic injuries: a French population-based study. *Hepatology* **36**, 451–455, <https://doi.org/10.1053/jhep.2002.34857> (2002).
38. Upadhyay, A. *et al.* Ibuprofen Induces Mitochondrial-Mediated Apoptosis Through Proteasomal Dysfunction. *Mol. Neurobiol.* **53**, 6968–6981, <https://doi.org/10.1007/s12035-015-9603-6> (2016).
39. Janssen, G. E. & Venema, J. F. Ibuprofen: Plasma Concentrations in Man. *J. Int. Med. Res.* **13**, 68, <https://doi.org/10.1177/030006058501300110> (1985).
40. Lecker, S. H., Goldberg, A. L. & Mitch, W. E. Protein degradation by the ubiquitin-proteasome pathway in normal and disease states. *J. Am. Soc. Nephrol.* **17**, 1807–1819, <https://doi.org/10.1681/ASN.2006010083> (2006).
41. Jamart, C. *et al.* Regulation of ubiquitin-proteasome and autophagy pathways after acute LPS and epoxomicin administration in mice. *BMC Musculoskelet. Disord.* **15**, 166, <https://doi.org/10.1186/1471-2474-15-166> (2014).
42. Ebstein, F., Kloetzel, P. M., Kruger, E. & Seifert, U. Emerging roles of immunoproteasomes beyond MHC class I antigen processing. *Cell. Mol. life sciences: CMLS* **69**, 2543–2558, <https://doi.org/10.1007/s00018-012-0938-0> (2012).
43. Launay, N. *et al.* Oxidative stress regulates the ubiquitin-proteasome system and immunoproteasome functioning in a mouse model of X-adrenoleukodystrophy. *Brain* **136**, 891–904, <https://doi.org/10.1093/brain/aws370> (2013).
44. Nesari, A., Mansouri, M. T., Khodayar, M. J. & Rezaei, M. Preadministration of high-dose alpha-tocopherol improved memory impairment and mitochondrial dysfunction induced by proteasome inhibition in rat hippocampus. *Nutr. Neurosci.* 1–11, <https://doi.org/10.1080/1028415X.2019.1601888> (2019).
45. Nguyen, A. *et al.* PKLR promotes colorectal cancer liver colonization through induction of glutathione synthesis. *J. Clin. Invest.* **126**, 681–694, <https://doi.org/10.1172/JCI83587> (2016).
46. Zanella, A., Fermo, E., Bianchi, P. & Valentini, G. Red cell pyruvate kinase deficiency: molecular and clinical aspects. *Br. J. Haematol.* **130**, 11–25, <https://doi.org/10.1111/j.1365-2141.2005.05527.x> (2005).
47. Kemmelmeier, F. S. & Bracht, A. Effects of the nonsteroidal anti-inflammatory drug mefenamic acid on energy metabolism in the perfused rat liver. *Biochemical pharmacology* **38**, 823–830, [https://doi.org/10.1016/0006-2952\(89\)90237-2](https://doi.org/10.1016/0006-2952(89)90237-2) (1989).
48. Garcia, M. *et al.* Phosphofructo-1-kinase deficiency leads to a severe cardiac and hematological disorder in addition to skeletal muscle glycogenosis. *PLoS Genet.* **5**, e1000615, <https://doi.org/10.1371/journal.pgen.1000615> (2009).
49. Mullarky, E. & Cantley, L. C. in *Innovative Medicine: Basic Research and Development* (eds. K. Nakao, N. Minato, & S. Uemoto) 3–23 (2015).
50. Schutt, F., Aretz, S., Auffarth, G. U. & Kopitz, J. Moderately reduced ATP levels promote oxidative stress and debilitate autophagic and phagocytic capacities in human RPE cells. *Invest. Ophthalmol. Vis. Sci.* **53**, 5354–5361, <https://doi.org/10.1167/iovs.12-9845> (2012).
51. Zhao, R. Z., Jiang, S., Zhang, L. & Yu, Z. B. Mitochondrial electron transport chain, ROS generation and uncoupling (Review). *Int. J. Mol. Med.* **44**, 3–15, <https://doi.org/10.3892/ijmm.2019.4188> (2019).
52. Bhatia, K., Elmarakby, A. A., El-Remessy, A. B. & Sullivan, J. C. Oxidative stress contributes to sex differences in angiotensin II-mediated hypertension in spontaneously hypertensive rats. *Am. J. Physiol. Regul. Integr. Comp. Physiol.* **302**, R274–282, <https://doi.org/10.1152/ajpregu.00546.2011> (2012).
53. Barp, J. *et al.* Myocardial antioxidant and oxidative stress changes due to sex hormones. *Braz. J. Med. Biol. Res.* **35**, 1075–1081, <https://doi.org/10.1590/s0100-879x2002000900008> (2002).
54. Johnson, T. A., Jinnah, H. A. & Kamatani, N. Shortage of Cellular ATP as a Cause of Diseases and Strategies to Enhance ATP. *Front. Pharmacol.* **10**, 98, <https://doi.org/10.3389/fphar.2019.00098> (2019).
55. Zheng, X. *et al.* Alleviation of neuronal energy deficiency by mTOR inhibition as a treatment for mitochondria-related neurodegeneration. *Elife* **5**, <https://doi.org/10.7554/eLife.13378> (2016).
56. Huang, H. *et al.* Physiological levels of ATP negatively regulate proteasome function. *Cell Res.* **20**, 1372–1385, <https://doi.org/10.1038/cr.2010.123> (2010).
57. Bolanos, J. P. Bioenergetics and redox adaptations of astrocytes to neuronal activity. *J. Neurochem.* **139**(Suppl 2), 115–125, <https://doi.org/10.1111/jnc.13486> (2016).
58. Seo, E., Kang, H., Choi, H., Choi, W. & Jun, H. S. Reactive oxygen species-induced changes in glucose and lipid metabolism contribute to the accumulation of cholesterol in the liver during aging. *Aging Cell* **18**, e12895, <https://doi.org/10.1111/acel.12895> (2019).
59. Porter, S. N., Howarth, G. S. & Butler, R. N. Non-steroidal anti-inflammatory drugs and apoptosis in the gastrointestinal tract: potential role of the pentose phosphate pathways. *Eur. J. Pharmacol.* **397**, 1–9, [https://doi.org/10.1016/s0014-2999\(00\)00237-5](https://doi.org/10.1016/s0014-2999(00)00237-5) (2000).
60. Kourounakis, A. P. *et al.* Experimental hyperlipidemia and the effect of NSAIDs. *Exp. Mol. Pathol.* **73**, 135–138, <https://doi.org/10.1006/exmp.2002.2449> (2002).
61. Chang, H. Y. *et al.* Clinical use of cyclooxygenase inhibitors impairs vitamin B-6 metabolism. *Am. J. Clin. Nutr.* **98**, 1440–1449, <https://doi.org/10.3945/ajcn.113.064477> (2013).
62. Reddy, J. K. & Hashimoto, T. Peroxisomal beta-oxidation and peroxisome proliferator-activated receptor alpha: an adaptive metabolic system. *Annu. Rev. Nutr.* **21**, 193–230, <https://doi.org/10.1146/annurev.nutr.21.1.193> (2001).
63. Furuta, E. *et al.* Fatty acid synthase gene is up-regulated by hypoxia via activation of Akt and sterol regulatory element binding protein-1. *Cancer Res.* **68**, 1003–1011, <https://doi.org/10.1158/0008-5472.CAN-07-2489> (2008).
64. Rashid, A. *et al.* Elevated expression of fatty acid synthase and fatty acid synthetic activity in colorectal neoplasia. *Am. J. Pathol.* **150**, 201–208 (1997).
65. Swinnen, J. V. *et al.* Overexpression of fatty acid synthase is an early and common event in the development of prostate cancer. *Int. J. Cancer* **98**, 19–22 (2002).
66. Milgraum, L. Z., Witters, L. A., Pasternack, G. R. & Kuhajda, F. P. Enzymes of the fatty acid synthesis pathway are highly expressed in *in situ* breast carcinoma. *Clin. Cancer Res.* **3**, 2115–2120 (1997).
67. Reddy, J. K. & Rao, M. S. Lipid metabolism and liver inflammation. II. *Fat. liver Dis. Fat. acid. oxidation. Am. J. Physiol. Gastrointest. Liver Physiol* **290**, G852–858, <https://doi.org/10.1152/ajpgi.00521.2005> (2006).
68. Kasuya, F., Hiasa, M., Kawai, Y., Igarashi, K. & Fukui, M. Inhibitory effect of quinolone antimicrobial and nonsteroidal anti-inflammatory drugs on a medium chain acyl-CoA synthetase. *Biochemical pharmacology* **62**, 363–367, [https://doi.org/10.1016/s0006-2952\(01\)00667-0](https://doi.org/10.1016/s0006-2952(01)00667-0) (2001).

69. Atshaves, B. P. *et al.* Liver fatty acid-binding protein and obesity. *J. Nutr. Biochem.* **21**, 1015–1032, <https://doi.org/10.1016/j.jnutbio.2010.01.005> (2010).
70. He, J. *et al.* Expression pattern of L-FABP gene in different tissues and its regulation of fat metabolism-related genes in duck. *Mol. Biol. Rep.* **40**, 189–195, <https://doi.org/10.1007/s11033-012-2048-3> (2013).
71. Fowler, C. J., Jonsson, K. O. & Tiger, G. Fatty acid amide hydrolase: biochemistry, pharmacology, and therapeutic possibilities for an enzyme hydrolyzing anandamide, 2-arachidonoylglycerol, palmitoylethanolamide, and oleamide. *Biochemical pharmacology* **62**, 517–526, [https://doi.org/10.1016/s0006-2952\(01\)00712-2](https://doi.org/10.1016/s0006-2952(01)00712-2) (2001).
72. Campos, S. P. *et al.* Expression of CYP1A1 and CYP1A2 in the liver and kidney of rabbits after prolonged infusion of propofol. *Exp. Toxicol. Pathol.* **68**, 521–531, <https://doi.org/10.1016/j.etp.2016.07.006> (2016).
73. Anzenbacher, P. & Anzenbacherova, E. Cytochromes P450 and metabolism of xenobiotics. *Cell. Mol. life sciences: CMLS* **58**, 737–747 (2001).
74. Hussain, T. *et al.* Induction of CYP1A1, CYP1A2, CYP1B1, increased oxidative stress and inflammation in the lung and liver tissues of rats exposed to incense smoke. *Mol. Cell Biochem.* **391**, 127–136, <https://doi.org/10.1007/s11010-014-1995-5> (2014).
75. Rademaker, M. Do women have more adverse drug reactions? *Am. J. Clin. Dermatol.* **2**, 349–351, <https://doi.org/10.2165/00128071-200102060-00001> (2001).
76. Lentini, E., Kasahara, M., Arver, S. & Savic, I. Sex differences in the human brain and the impact of sex chromosomes and sex hormones. *Cereb. Cortex* **23**, 2322–2336, <https://doi.org/10.1093/cercor/bhs222> (2013).
77. Beery, A. K. Inclusion of females does not increase variability in rodent research studies. *Curr. Opin. Behav. Sci.* **23**, 143–149, <https://doi.org/10.1016/j.cobeha.2018.06.016> (2018).
78. Carrel, L. & Willard, H. F. X-inactivation profile reveals extensive variability in X-linked gene expression in females. *Nat.* **434**, 400–404, <https://doi.org/10.1038/nature03479> (2005).
79. Becker, J. B. *et al.* Strategies and methods for research on sex differences in brain and behavior. *Endocrinol.* **146**, 1650–1673, <https://doi.org/10.1210/en.2004-1142> (2005).
80. Shi, L. X. *et al.* Hepatic Cyp1a2 Expression Reduction during Inflammation Elicited in a Rat Model of Intermittent Hypoxia. *Chin. Med. J.* **130**, 2585–2590, <https://doi.org/10.4103/0366-6999.217084> (2017).
81. Finnstrom, N., Ask, B., Dahl, M. L., Gadd, M. & Rane, A. Intra-individual variation and sex differences in gene expression of cytochromes P450 in circulating leukocytes. *Pharmacogenomics J.* **2**, 111–116, <https://doi.org/10.1038/sj.tpj.6500086> (2002).
82. Kojima, M. *et al.* IL-1 regulates the Cyp7a1 gene and serum total cholesterol level at steady state in mice. *Biochem. Biophys. Res. Commun.* **379**, 239–242, <https://doi.org/10.1016/j.bbrc.2008.12.032> (2009).
83. Shao, F. *et al.* Expression of miR-33 from an SREBP2 intron inhibits the expression of the fatty acid oxidation-regulatory genes CROT and HADHB in chicken liver. *Br. Poult. Sci.* **60**, 115–124, <https://doi.org/10.1080/00071668.2018.1564242> (2019).
84. Violante, S. *et al.* Peroxisomes contribute to the acylcarnitine production when the carnitine shuttle is deficient. *Biochim. Biophys. Acta* **1831**, 1467–1474, <https://doi.org/10.1016/j.bbalip.2013.06.007> (2013).
85. Perspicace, E. *et al.* Novel, potent and selective 17 β -hydroxysteroid dehydrogenase type 2 inhibitors as potential therapeutics for osteoporosis with dual human and mouse activities. *Eur. J. Med. Chem.* **83**, 317–337, <https://doi.org/10.1016/j.ejmech.2014.06.036> (2014).
86. Salah, M., Abdelsamie, A. S. & Frotscher, M. Inhibitors of 17 β -hydroxysteroid dehydrogenase type 1, 2 and 14: Structures, biological activities and future challenges. *Mol. Cell Endocrinol.* **489**, 66–81, <https://doi.org/10.1016/j.mce.2018.10.001> (2019).
87. Bagi, C. M., Wood, J., Wilkie, D. & Dixon, B. Effect of 17 β -hydroxysteroid dehydrogenase type 2 inhibitor on bone strength in ovariectomized cynomolgus monkeys. *J. Musculoskelet. Neuronal Interact.* **8**, 267–280 (2008).

Author contributions

S.T. and A.G. conceived the ideas for the work and contributed to the design of the experimental protocols, analysis of the results, data interpretation, manuscript writing and revised the manuscript with input from all co-authors. S.T. and M.M. performed Western blotting experiments and biological assays, statistical analysis and interpretation of data. J.N. performed biological assays and data analysis. M.R.S. and B.P. did mass spectrometry and B.P. and A.G. performed data analysis. All authors critically reviewed and finally approved the manuscript.

Competing interests

The authors declare no competing interests.

Additional information

Supplementary information is available for this paper at <https://doi.org/10.1038/s41598-020-60053-y>.

Correspondence and requests for materials should be addressed to A.V.G.

Reprints and permissions information is available at www.nature.com/reprints.

Publisher's note Springer Nature remains neutral with regard to jurisdictional claims in published maps and institutional affiliations.



Open Access This article is licensed under a Creative Commons Attribution 4.0 International License, which permits use, sharing, adaptation, distribution and reproduction in any medium or format, as long as you give appropriate credit to the original author(s) and the source, provide a link to the Creative Commons license, and indicate if changes were made. The images or other third party material in this article are included in the article's Creative Commons license, unless indicated otherwise in a credit line to the material. If material is not included in the article's Creative Commons license and your intended use is not permitted by statutory regulation or exceeds the permitted use, you will need to obtain permission directly from the copyright holder. To view a copy of this license, visit <http://creativecommons.org/licenses/by/4.0/>.

© The Author(s) 2020